Thermal Conductance

Figure 5 shows the variation of specific conductance of the cone to flat joints with applied load, for two different cone angles and two different combinations of joint materials. In all cases, the agreements between the measured thermal conductances and predicted values (based on analog or numerical solutions) are good. In each case, the support pressure was taken from physical testing of the material, typically as shown in Fig. 4. The thermal testing indicated no effect of strain hardening changing the local thermal conductivity of the contact materials.

Conclusions

As a result of the physical and thermal tests on compressed cone to flat metallic contacts it is possible to predict the thermal conductance of this type of joint with confidence. Parameters required for these predictions include the shape of the deformed joint whilst loaded, and the true support pressure. The latter varies with the initial cone angle, and is always less than the Meyer Hardness of the material of the conical element. The anomalies of previous work[4] based on simpler physical models and on assumed values of support pressure equal to the Meyer Hardness have been resolved.

The electrical analogue proved particularly useful for rapid determinations of joint conductances of many shapes of contact, giving good agreement with computer predictions based on constant physical properties of the joint materials. Both of these methods produced results in good agreement with thermal conductance measurements, for a variety of cone angles and joint materials.

References

[1] Cetinkale, T. N. and Fishenden, M., "Thermal Conductance of Metallic Surfaces in Contact," General Discussion on Heat Transfer, I. Mech. E. London, 1951, pp. 271-275.

[2] Clausing, A. M. and Chao, B. T., "Thermal Contact Resistance in a Vacuum Environment," *Journal of Heat Transfer,* ASME, Ser. C, Vol. 87, 1965, pp. 243-251.

[3] Kitsha, W. W. and Yovanovich, M. M., "Experimental Investigation on the Overall Thermal Resistance of Sphere-Flat Contacts," *AIAA Progress in Astronautics and Aeronautics: Heat Transfer with Thermal Control Applications,* Vol. 39, edited by M. Michael Yovanovich, MIT Press, Cambridge, Mass., 1975, pp. 93-110.

[4] Williams, A., "Heat Flow Through Single Points of Metallic Contacts of Simple Shapes," *AIAA Progress in Astronautics and Aeronautics: Heat Transfer with Thermal Control Applications,* Vol. 39, edited by M. Michael Yovanovich, MIT Press, Cambridge, Mass., 1975, pp. 129-142.

[5] Mallock, A., "Hardness," *Nature,* No. 2934, Vol. 117, 1926, pp. 117-118.

[6] Hill, R., *The Mathematical Theory of Plasticity,* Oxford University Press, N.Y., 1967.

[7] Bowden, F. P. and Tabor, D., *The Friction and Lubrication of Solids,* Part 1, Oxford University Press, N.Y., 1950.

Interaction Effects of Multiple Cracks

T.M. Hsu* and J.W. Markham†
Lockheed-Georgia Company, Marietta, Ga.

I. Introduction

THE application of fracture mechanics to fatigue-crack growth and residual-strength analyses has resulted in much progress during the last decade. Yet the presence of cracks in engineering structures still poses many serious research problems that have to be solved. One such problem is the interaction of multiple cracks originating at fastener holes.

Fatigue cracks usually originate in the regions of high stress concentration, which exist notwithstanding careful detail-design procedures. Hardly any assembled structure, such as fastener holes and access holes, is free of geometric discontinuities. A review of U.S. Air Force aircraft structural failures[1] revealed that cracks emanating from fastener holes represent the most common origin of these failures.

To date, there has been much useful work done on the problem of determining reliable stress-intensity factors for cracks emanating from fastener holes. Almost all of these analytical determinations are based upon modifications of a solution obtained by Bowie[2] for cracks emanating from a circular hole in an infinite elastic sheet. The problem of the interaction effects of periodic parallel straight cracks having the same crack length has been investigated.[3,4] But the interaction effects of cracks originating at a multiplicity of fastener holes has not been sufficiently studied.

In order to minimize the test time and cost, and to gather the maximum amount of useful data, specimens containing multiple cracks have been extensively employed in experimental fracture mechanics programs. Unless the crack lengths are small and/or the spacing between cracks is relatively large, interaction between cracks will occur, and the data generated under such test, if not meaningless, may be very difficult to analyze because current analytical methodology is not able to account for such an interaction. The purpose of this study was to investigate the effect of the additional cracked hole or holes on the stress-intensity factor of a primary crack.

II. Analysis and Discussion

To investigate the interaction effects between the cracks emanating from fastener holes, the finite-element method was used to compute the stress-intensity factors for the typical cracked geometry shown in Fig. 1. Due to symmetry, it was necessary to model only the first quadrant of the plate. A detail of the two-dimensional finite-element model is shown in Fig. 2. The model consists of 325 nodes and 525 constant-strain triangular elements. The crack-tip regions in the finite-element model were represented by eight-node and ten-node singularity elements developed at Lockheed-Georgia[5] for the purpose of computing the stress-intensity factors appropriate to various crack lengths. A detailed discussion of these singularity elements is given in Ref. 5.

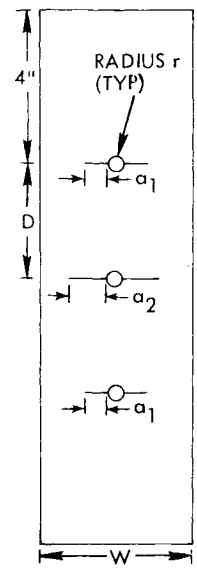

Fig. 1 Specimen geometry.

Presented at the AIAA/ASME/SAE 17th Structures, Structural Dynamics and Materials Conference, King of Prussia, Pa., May 5-7, 1976 (in bound volume of Conference papers, no paper number); submitted June 4, 1976; revision received Nov. 17, 1976.

Index categories: Aircraft Structural Design; Structural Static Analysis.

*Aircraft Development Engineer-Specialist, Advanced Structures Department. Member AIAA.

†Aircraft Structures Engineer-Senior, Advanced Structures Department.

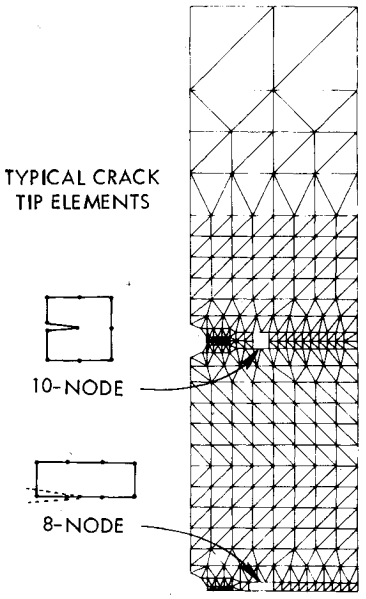

Fig. 2 Finite-element model.

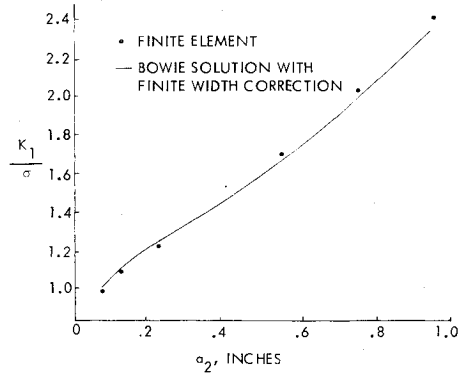

Fig. 3 Normalized stress intensity factor of primary crack with the absence of an additional crack.

Let a_1 denote the crack length at the outer holes and a_2 the crack length at the inner hole. All holes have the same diameter, $2r$; D is the spacing between the outer and inner holes; W is the width of the plate. The stress-intensity factor per unit far-field uniform stress was computed for a double-crack emanating from the inner hole and with no cracks at the outer holes. The computed stress-intensity factor normalized by the uniform far-field stress is shown in Fig. 3 for $r=0.2$ in., $D=3$ in. and $W=4$ in. Bowie's solution with the appropriate finite-width correction is included for comparison.

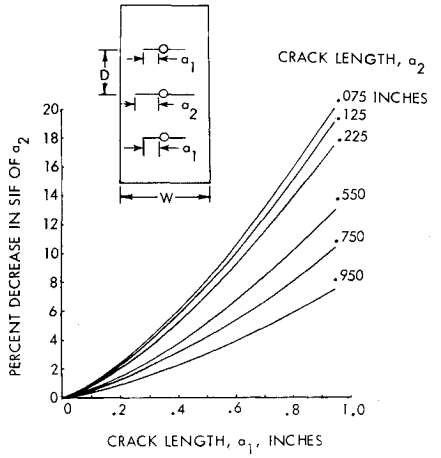

Fig. 4 The percent decrease in the SIF of a_2 due to the presence of a_1.

As can be seen, the computed stress-intensity factor is within 3 percent of the modified Bowie solution for a_2 ranging from 0.075 in. to 0.950 in. These results provide a baseline data for studying the effect of additional crack(s) on the stress-intensity factor of the primary crack.

To determine the change in the stress-intensity factor of the inner crack, a_2, due to the presence of outer cracks, a_1, the crack length a_1 was changed from 0.075 in. to 0.950 in. for each a_2 and the computed stress-intensity factor for a_2 is tabulated in Table 1. The number inside the parenthesis indicates the percent decrease in the stress-intensity factor from the baseline value. These results are shown in Fig. 4. As seen from Fig. 4, for a given constant crack length a_2, the stress-intensity factor of the inner crack decreases (or percentage increases) with the increase of crack length a_1; and for a constant crack length a_1, the percentage change in the stress-intensity factor of a_2 decreases when the crack length a_2 increases. For example, for $a_1=0.95$ in., the percent decrease in K_1 for a_2 changes from 20% to 7.4% when a_2 changes from 0.075″ to 0.95″. The result indicates that the effect of the outer crack on K_1 for the inner crack is more severe when a_2 is small. This is because the effective load transferred through the uncracked net section of the outer hole to the tip of the inner crack decreases with the increase of a_1 and the decrease of a_2, unless the hole spacing is large enough to prohibit the interaction. Similar results on the change in the stress-intensity factor of the outer crack, a_1, due to the presence of the inner crack, a_2, are shown in Fig. 5. By comparing the results shown in Figs. 4 and 5, one can see that the effect of a_1 on K_1 for a_2 is twice the effect of a_2 on K_1 for a_1.

Table 1 Normalized stress-intensity factor, K_1/σ, for various inner-crack lengths

Inner-crack length a_1, in.	K_1/σ For a_2 with $a_2=$, in.					
	0.075	0.125	0.225	0.550	0.750	0.950
0	0.960 (0)[a]	1.060 (0)	1.196 (0)	1.691 (0)	2.022 (0)	2.417 (0)
0.075	0.954 (−0.65)	1.054 (−0.62)	1.189 (−0.58)	1.684 (−0.42)	2.015 (−0.34)	2.411 (−0.24)
0.125	0.948 (−1.3)	1.047 (−1.2)	1.182 (−1.1)	1.677 (−0.83)	2.009 (0.65)	2.406 (−0.47)
0.225	0.934 (−2.7)	1.033 (−2.6)	1.168 (−2.3)	1.662 (−1.7)	1.994 (−1.4)	2.393 (−0.98)
0.550	0.871 (−9.2)	0.967 (−8.8)	1.100 (−8.0)	1.590 (−5.9)	1.928 (−4.7)	2.336 (−3.4)
0.750	0.822 (−14.4)	0.916 (13.6)	1.047 (12.5)	1.534 (−9.3)	1.874 (−7.3)	2.290 (−5.3)
0.950	0.767 (−20.0)	0.859 (−19.0)	0.988 (−17.4)	1.472 (−13.0)	1.814 (−10.3)	2.238 (−7.4)

[a] Number inside the parenthesis indicates the percent difference from the baseline ($a_1=0$).

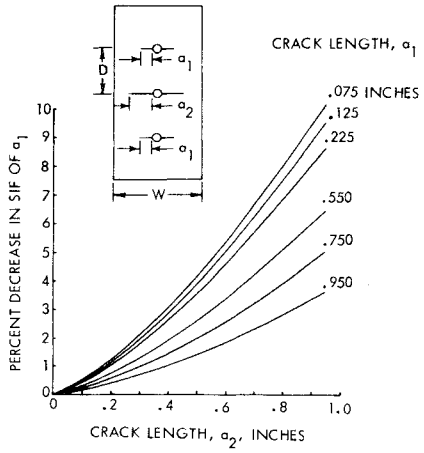

Fig. 5 The percent decrease in the SIF of a_1 due to the presence of a_2.

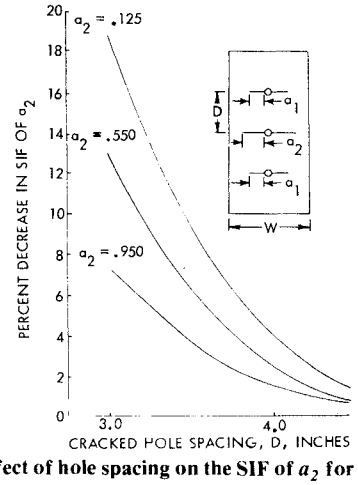

Fig. 6 Effect of hole spacing on the SIF of a_2 for $a_1 = 0.95$ in.

By idealizing the hole as a straight crack of length $2r$, the computed normalized stress-intensity factors for $a_1 = a_2$ are compared with those of periodic parallel straight cracks in Table 2 for a crack spacing to plate width ratio of 0.75. As anticipated, the current computed values are higher than those of Ref. 3 for a short crack length due to local effect of the hole. For a crack length longer than 2 times the hole diameter, the effect of the hole is negligible and hence the current analysis gives the same values as those of equivalent straight cracks.

The effect of the hole spacing on changes of stress-intensity factor has also been studied. Typical results on the percentage changes in K_1 for a_2 are shown in Fig. 6 as a function of hole spacing for $a_1 = 0.95$ in. and various values of a_2. As seen from this figure, the percentage change in the K_1 for a_2 decreases rapidly as the crack spacing increases. For $D = 3$ in. and $a_2 = 0.125$ in., K_1 for a_2 (with $a_1 = 0.95$ in.) is 19% less

Table 2 Comparison of current result with that of periodic parallel straight cracks (Ref. 3)

Equivalent crack length $\bar{a} = a + r$, $r = 0.2$	$K_1/\sigma\sqrt{\pi\bar{a}}$	
	Current analysis	Ref. 3 ($D = 0.75w$)
0.275	1.03	1.0
0.325	1.04	1.0
0.025	1.01	1.01
0.750	1.04	1.03
0.950	1.08	1.08
1.150	1.18	1.18

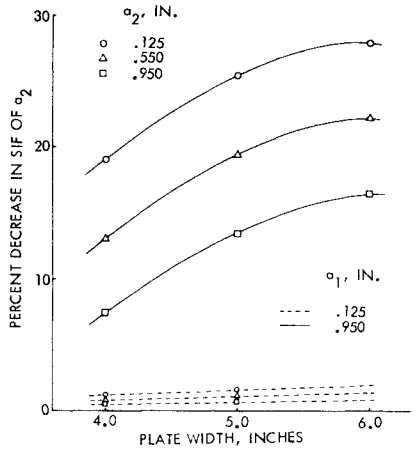

Fig. 7 Effect of plate width on the SIF of a_2.

than the case where the outer crack a_1 is absent. However, when D increases from 3 in. to 4.5 in., the difference decreases from 19% to 1.4%. Physically, it means that the interaction effect is negligible when the hole spacing is greater than 4.5 in. for the particular plate geometry studied.

To study the effect of the width of the plate on the interaction of cracked holes, the basic model was widened to 5 and 6 in. respectively, while the hole spacing was maintained at 3 in. The results expressed as percentage reductions in the stress-intensity factor for a_2 are shown in Fig. 7 as a function of the plate width for various values of a_1 and a_2. For constant crack lengths (both a_1 and a_2) and fixed hole spacing, the reduction in the stress-intensity factor for a_2 increases with the increasing plate width. When the crack length a_1 is small, say 0.125 in., the effect of the width on the change of K_1 for a_2 is negligible. However, as a_1 increases, the width effect on the changes of the stress-intensity factor for a_2 becomes more significant. For instance, for $a_1 = 0.95$ in. and $a_2 = 0.125$ in., the percent decrease in K_1 for a_2 changes from 19 percent to 28 percent when the width of the plate increases from 4 in. to 6 in.

III. Conclusion

The finite-element method with the inclusion of high-order singularity elements has been used to study the effect of surrounding crack(s) on the stress-intensity factor of a primary crack. Based on the study conducted, the following conclusions have been observed:

1) The stress-intensity factor of the primary crack decreases when additional crack(s) are present.

2) For identical hole conditions and crack lengths, the effect of a_1 on K_1 for a_2 is twice the effect of a_2 on K_1 for a_1.

3) The interaction effect between cracks decreases rapidly with increased vertical spacing.

4) For fixed crack lengths and hole spacings, the interaction effect increases when the plate width increases.

5) The interaction is most significant when one of the cracks is much larger than the other. In such a case, the stress-intensity factor for a shorter crack will be much lower than the corresponding value obtained without the additional crack. The effect of a shorter crack on the stress intensity factor of a longer crack is minimum.

6) For a 4 in. wide specimen, if the hole spacing is 3 in., the maximum crack length (both a_1 and a_2) without practical load interaction (less than 2 percent reduction in the K_1) is about 0.4 in. measured from the center of the 0.4 in. diameter hole. However, if the hole spacing is increased to 4.5 in., the maximum crack length without practical load interaction is about 1.1 in.

Although only double-cracks emanating from an open hole were studied here, the analysis can be easily extended to study the single-crack geometry or cracks emanating from close-

tolerance fastener holes with and without fastener-load transfer.

References

[1]Gran, R.J., Orazio, F.D., Paris, P.C., Irwin, G.R., and Hertzberg, R., "Investigation and Analysis Development of Early Life Aircraft Structural Failures," Air Force Flight Dynamics Lab, Wright Patterson AFB, Ohio, AFFDL-TR-70-149, March, 1971.

[2]Bowie, O.L., "Analysis of Infinite Plate Containing Radial Cracks Originating from a Circular Hole," *Journal of Mathematics and Physics*, Vol. 23, April 1956, pp. 60-71.

[3]Isida, M., "Effect of Width and Length on Stress Intensity Factors of Internally Cracked Plates Under Various Boundary Conditions," *International Journal of Fracture Mechanics*, Vol. 7, Sept. 1971, pp. 301-316.

[4]Tada, H., Paris, P.C., and Irwin, G.R., *The Stress Analysis of Cracks Handbook*, Del Research Corporation, Hellerstown, Pa., 1973, p. 14.1.

[5]Aberson, J.A. and Anderson, J.M., "Cracked Finite-Elements Proposed for NASTRAN," *Third NASTRAN User's Colloquium*, NASA TMX-2893, 1973, pp. 531-550.

A Simplified Algorithm for Determining the Stability of Linear Systems

Dewey H. Hodges
Ames Directorate, U.S. Army Air Mobility R&D Lab., Moffett Field, Calif.

Introduction

IN aeroelasticity, as well as in other nonconservative problems in the theory of elastic stability, there is often a need for information concerning the stability of small motions about an equilibrium state. Such analyses can generally be reduced to standard eigenvalue problems with a host of well-known methods of solution. The eigenvalues may provide too much information, however. The analyst may only want to know whether the motion is stable. To determine the stability for a system of n equations of order r by classical methods first requires extracting $N=nr$ eigenvalues and then testing each real part to see if it is positive (unstable) or negative (stable). A scheme that requires calculation of only one number to be tested would be clearly superior, especially if the computation time was less than that of extracting eigenvalues. Such a scheme has been developed and is the subject of this paper.

Analysis

We assume that the equations of motion may be reduced to the eigenvalue problem

$$Px=\lambda x$$

where P is the stability matrix, x is the vector of system generalized coordinates, and λ is the set of eigenvalues. The matrix P is real and of order $N\times N$. Extracting the eigenvalues is quite straightforward, but if the stability of the system is the extent of our concern then we should take a different approach.

We first should reduce P to an upper Hessenberg matrix H by so-called similarity transformations.[1] This step is available in many standard subroutine packages (e.g., Refs. 2 and 3). The form of H is

$$H=\begin{bmatrix} h_{1,1} & h_{1,2} & h_{1,3} & \cdots & h_{1,N-1} & h_{1,N} \\ k_2 & h_{2,2} & h_{2,3} & \cdots & h_{2,N-1} & h_{2,N} \\ 0 & k_3 & h_{3,3} & \cdots & h_{3,N-1} & h_{3,N} \\ \cdot & \cdot & \cdot & & \cdot & \cdot \\ \cdot & \cdot & \cdot & & \cdot & \cdot \\ 0 & 0 & 0 & \cdots & k_N & h_{N,N} \end{bmatrix}$$

The next step is to generate the characteristic polynomial. The method of Leverrier[4] is often used. The method used here[5] is more efficient than Leverrier's method, which requires about N times as many multiplications. If we denote by $p_r(\lambda)$ the characteristic polynomial of the square submatrix H_r of order r, then expanding $\det(H_r-\lambda I)$ in terms of its rth column yields

$$p_0(\lambda)=1$$

$$p_1(\lambda)=h_{1,1}-\lambda$$

$$p_r(\lambda)=(h_{r,r}-\lambda)p_{r-1}(\lambda)-h_{r-1,r}k_r p_{r-2}(\lambda)$$
$$+h_{r-2,r}k_r k_{r-1}p_{r-3}(\lambda)-\ldots$$
$$+(-1)^{r-1}h_{1,r}k_r k_{r-1}\ldots k_2 p_0(\lambda)$$

To derive the coefficients of $p_N(\lambda)$, we must store those of $p_r(\lambda)$ for $r=1, 2,\ldots,N-1$. The coefficients of $p_N(\lambda)$ are denoted by c_i, where $c_1=(-1)^N$ and

$$\sum_{i=1}^{N+1} c_i\lambda^{N-i+1}=0$$

A Fortran coding for this part of the numerical scheme may be obtained from the author.

The stability of the system may be determined by the Routh-Hurwitz criterion.[6] The conditions for instability are

$$c_{N+1}<0 \quad \text{(divergence)}$$

or

$$\Delta_{N-1}< \quad \text{(flutter)}$$

where

$$\Delta_{N-1}=\begin{vmatrix} c_2 & c_4 & c_6 & \cdots & c_{2N-2} \\ c_1 & c_3 & c_5 & \cdots & c_{2N-3} \\ 0 & c_2 & c_4 & \cdots & c_{2N-4} \\ 0 & c_1 & c_3 & \cdots & c_{2N-5} \\ \cdot & \cdot & \cdot & & \cdot \\ \cdot & \cdot & \cdot & & \cdot \\ \cdot & \cdot & \cdot & & \cdot \\ 0 & 0 & & & c_N \end{vmatrix}$$

and $c_i=0$ for $i>N+1$. Any convenient scheme for evaluating the determinant Δ_{N-1} may be used such as the LU decomposition. It would be faster, however, to take advantage of the form of Δ_{N-1} as discussed in Ref. 6. The computation of $c_i, i=1, 2,\ldots,N+1$ and of Δ_{N-1}, combined, requires fewer multiplications than calculating all the eigenvalues (even using the slower LU decomposition to evaluate Δ_{N-1} as is done in the numerical example below, and the dynamic stability (flutter) is known by simply checking the sign of one number. The static stability (divergence) can be more efficiently determined from a static criterion alone without introducing dynamic effects. A combination of this scheme and linear interpolation provides rapid convergence to a stability boundary indicated by a change in sign of Δ_{N-1}. This

Received June 29, 1976; revision received Nov. 23, 1976.
Index categories: Aeroelasticity and Hydroelasticity; Structural Dynamic Analysis.

*Research Scientist, Army Aeronautical Research Group. Member AIAA.